Journal of Physics and Chemistry of Solids 211 (2026) 113407

Contents lists available at ScienceDirect

Journal of Physics and Chemistry of Solids

journal homepage: www.elsevier.com/locate/jpcs

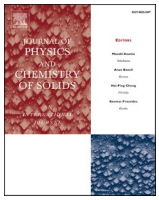

Charge transport mechanism in boron-irradiated Si_3N_4

V.A. Gritsenko [a,b], Yu N. Novikov [a], A.A. Gismatulin [a,*]

[a] Rzhanov Institute of Semiconductor Physics SB RAS, 13 Lavrentiev aven., 630090, Novosibirsk, Russia
[b] Novosibirsk State Technical University, 20 Marx aven, 630073, Novosibirsk, Russia

ARTICLE INFO

Keywords:
Irradiation
Annealing
Dielectric
Computer simulations
Transport properties

ABSTRACT

The effect of 100 keV boron ion irradiation with different fluences on the charge transport in amorphous Si_3N_4 is studied in the paper. The irradiation of Si_3N_4 leads to an increase in leakage currents by approximately three orders of magnitude. The charge transport in the initial (before irradiation) Si_3N_4 sample is satisfactorily described by the multiphonon isolated trap ionization mechanism. After irradiation with ions, the charge transport in Si_3N_4 is limited by the phonon-assisted tunneling between neighboring traps. An increase in the leakage current in ion-irradiated Si_3N_4 is due to an increase in the trap concentration and a decrease in the trap energy. Annealing irradiated Si_3N_4 sample leads to a decrease in the leakage currents to that of the initial Si_3N_4 sample. The ionization trap energy in the initial Si_3N_4 and irradiated and annealed Si_3N_4 lies in the range from 1.5 eV to 1.6 eV. An increase in the leakage currents after the ion irradiation in Si_3N_4 is explained by the radiation defect formations.

1. Introduction

Ion doping (ion implantation) is widely used for doping and controlling the semiconductor conductivity [1,2]. Generally, ions are implanted into a semiconductor through a dielectric layer, such as silicon oxide (SiO_2) or silicon nitride (Si_3N_4). When ions are implanted through a dielectric, radiation defects are formed upon irradiation. In semiconductors, the charge transport is carried out by free carriers [3]. In dielectrics, the charge transport is usually carried out through traps [3–7].

SiO_2 and Si_3N_4 are the key dielectrics in microelectronics [3]. Currently, the Frenkel mechanism of the trap ionization model is widely used to describe the charge transport in dielectrics [3,8,9]. Recently, the charge transport in dielectrics of semiconductor devices has been described by multiphonon trap ionization [10,11]. At a low trap concentration, ionization occurs in the conduction band (Makram-Ebeid and Lannoo model) [10–13]. At a high trap concentration, an electron tunnels to a neighboring trap (Nasyrov-Gritsenko model [10,11,14]).

The trap nature (atomic and electronic structure) responsible for the charge localization and transport in amorphous Si_3N_4 is the subject of intensive research. Paramagnetic defects, a nitrogen atom with an unpaired electron [15], a triply coordinated silicon atom with an unpaired electron [16–20] and a polaron model of capture on a diamagnetic Si–Si defect [21–23] are considered.

Amorphous Si_3N_4 is used as a storage medium in modern TANOS (TaN–Al_2O_3–Si_3N_4–SiO_2–Si) charge trap flash (CTF) memories [24,25]. The TANOS CTF operation principle is based on the localization of electrons and holes on deep traps in Si_3N_4. When a negative or positive potential is applied to the TaN gate, holes or electrons tunnel through the SiO_2 compound and are captured on traps in Si_3N_4. Holes localized in Si_3N_4 induce a conductive inversion channel in silicon (logical “1”). When holes accumulate in Si_3N_4, the inversion channel disappears (logical “0”). The maximum number of CTF reprogramming cycles is 10^4 and the response time in the reprogramming mode is 1 ms. The information storage time in a TANOS CTF is 10 years at 85 °C.

The study of the ion irradiation effect on the dielectric conductivity is of scientific and practical interest. Irradiation and implantation of dielectrics with various ions was studied in Refs. [1,2,26–31]. In Ref. [26], it was shown that the implantation of B or P ions into Si_3N_4 leads to the trap formation that can capture a charge. In Ref. [27], it was shown that the implantation of N^+ ions into the gate dielectric leads to the formation of electron traps in it. In Ref. [31], it was shown that proton-irradiation of Si_3N_4 leads to an increase in the leakage current. The aim of this work is to study the B^+ ion irradiation effect on the charge transport mechanisms in Si_3N_4.

* Corresponding author.
E-mail address: aagismatulin@isp.nsc.ru (A.A. Gismatulin).

https://doi.org/10.1016/j.jpcs.2025.113407
Received 15 September 2025; Received in revised form 13 November 2025; Accepted 26 November 2025
Available online 29 November 2025

2. Experimental process

Amorphous Si_3N_4 films were synthesized by the chemical vapor deposition method from a mixture of silane SiH_4 and ammonia NH_3 at 850 °C at the ratio $SiH_4/NH_3 = 1:100$. To study the charge transport, a 100 nm thick Si_3N_4 film was deposited on n-type silicon with orientation (100). The thickness and refractive index were estimated using an ellipsometer at a wavelength of 632.8 nm. Si_3N_4 was irradiated with boron (B^+) ions in the ion beam implanter IBS IMC200. Ion beam implanter IBS IMC200 was used in the scanning method to reduce the non-uniformity of irradiation over the sample area. The irradiated energy of 100 keV ions was chosen such that B^+ ions flew past Si_3N_4, i.e. the B^+ ions were distributed in silicon. The B^+ ion irradiation was used instead of implantation to create defects in Si_3N_4. The STRIM-2013 program was used to calculate Si and N vacancies and the distribution of irradiated B^+ in the Si_3N_4/Si-substrate system (Fig. 1) to choose the B^+ irradiation energy. The Si_3N_4 layer was set with the density of 3.44 g/cm^3. An additional 500 nm thick silicon substrate layer was added for the calculation. The irradiation of 10000 B^+ ions was calculated at the energy of 100 keV with the irradiation angle of 0°. The calculation results are shown in Fig. 1. Calculated number of vacancies per incident ion *versus* depth in Fig. 1(a). Taking into account the irradiation fluence 3×10^{15} ion/cm^{-2} and the 100 nm layer thickness, the concentration of generated nitrogen and silicon vacancies in the Si_3N_4 layer are around 10^{22} cm^{-3}. The distribution of B^+ in Si_3N_4 after the ion irradiation at the ion energy 100 keV and the irradiation fluence 3×10^{15} ion/cm^{-2} is shown in Fig. 1(b). The irradiation fluences were 3×10^{12} ion/cm^2, 3×10^{14} ion/cm^2 and 3×10^{15} ion/cm^2. The annealing of irradiated Si_3N_4 was carried out in a nitrogen atmosphere at 700 °C for 30 min. The upper aluminum contacts were deposited through a shadow mask by thermal sputtering. The Al upper contact area was 5×10^{-3} cm^2. The bottom electrode contact was deposited without shadow mask by thermal sputtering.

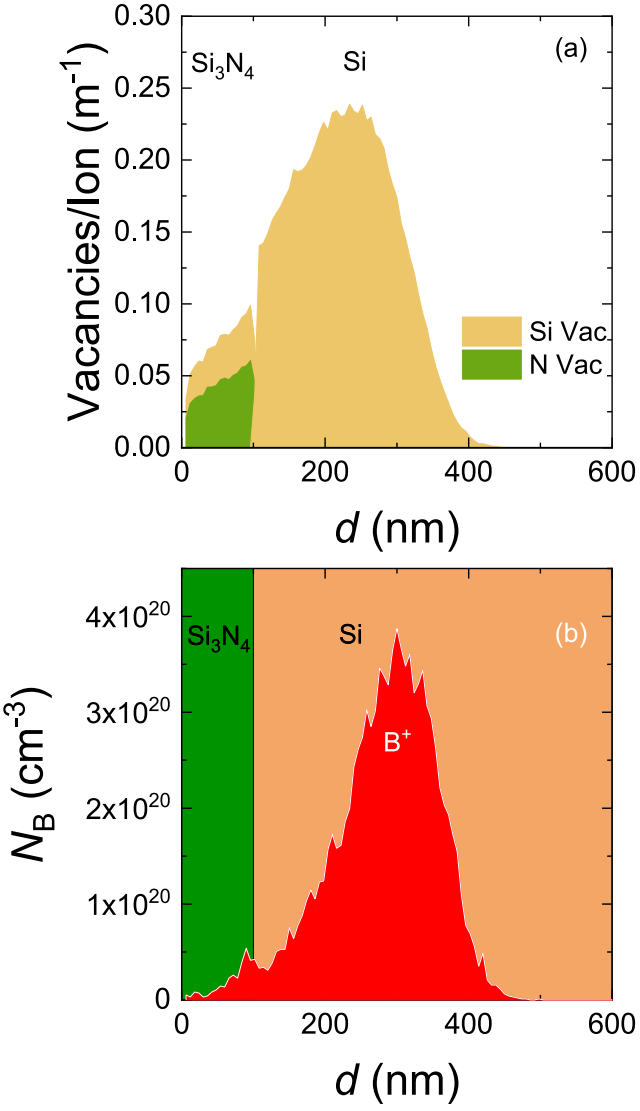

Fig. 1. (a) Calculated number of vacancies per incident ion *versus* depth. (b) The distribution of B^+ in Si_3N_4 after the ion irradiation at energy 100 keV and the fluence 3×10^{15} ion/cm^{-2}.

3. Results and discussion

The experimental **X-ray photoelectron spectroscopy (XPS)** spectra of Si 2s at the atomic level (circles) for Si, Si_3N_4 implanted with B^+ ions (irradiation fluence is 3×10^{14} ion/cm^{-2}), the initial Si_3N_4 film, and the deconvolution of these spectra (dashed line) are shown in Fig. 2. The B^+ ion irradiation into SiN_x is accompanied by broadening and a shift of the Si 2s spectrum toward lower energies (Fig. 2). When calculating the Si 2s spectra, it was assumed that five $SiN_\nu Si_{4-\nu}$ tetrahedra (where ν = 0,1,2,3,4) contribute to the Si 2s spectrum and these contributions are presented as a sum of Gaussian and Lorentzian (GL) functions. First, the energy position (E_ν) and the width (σ_ν) of the Si 2s state for Si ($SiSi_4$ tetrahedron) were determined: $E_0 = 151$ and $\sigma_0 = 2$ eV [32]; for Si_3N_4 (SiN_4 tetrahedron): $E_4 = 152.6$ and $\sigma_4 = 2.8$ eV [33]. The positions and widths of the intermediate, three GL functions of Si 2s states (E_ν and σ_ν where $\nu = 1, 2, 3$), for $SiNSi_3$ SiN_2Si_2 $SiNSi_3$ tetrahedra, were determined by the linear interpolation of values $E_0(\sigma_0)$, $E_4(\sigma_4)$ using the number of silicon atoms as a parameter. The deconvolution of the Si 2s spectra was performed using the formula [34]:

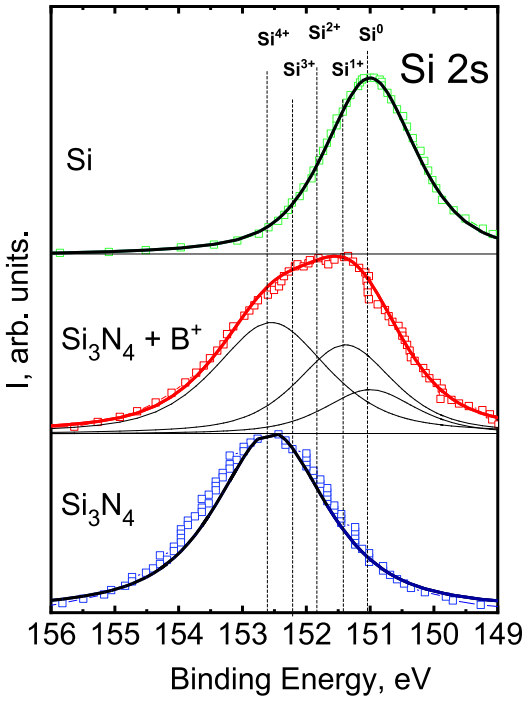

Fig. 2. Experimental XPS spectra of the level (squares) for ion-implanted Si and the initial Si_3N_4 film, and their deconvolution (solid lines). Notations Si^{4+}, Si^{3+}, Si^{2+}, Si^{1+} and Si^0 indicate the contributions to the Si 2s spectrum from five $SiN_\nu Si_{4-\nu}$ tetrahedra, where $\nu = 0, 1, 2, 3, 4$. The irradiation fluence is 3×10^{14} ion/cm^{-2}.

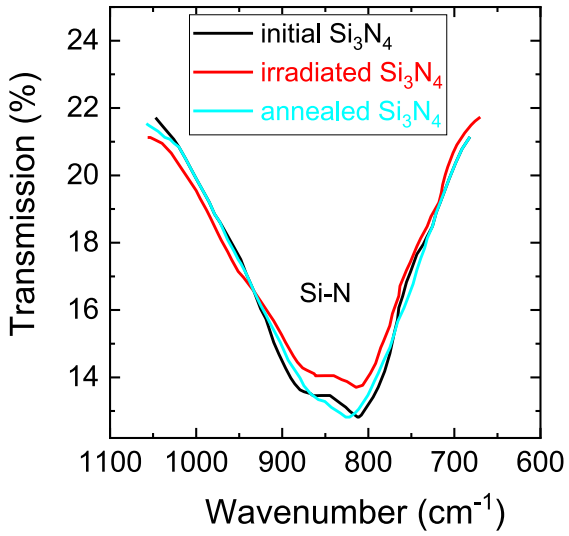

Fig. 3. Infrared transmission spectrum of the initial Si_3N_4 film, and Si_3N_4 films irradiated with B^+ ions (fluence 3×10^{14} ion/cm^{-2}) before and after the subsequent annealing.

$$I(E) = \sum_{\nu=0}^{4} W_\nu \left[(1-\chi)\exp\left(\frac{-4\ln(2)(E-E_\nu)^2}{\sigma_\nu^2}\right) + \frac{\chi}{1+4\frac{(E-E_\nu)^2}{\sigma_\nu^2}} \right], \quad (1)$$

where *I(E)* is the calculated spectrum, *E* is the energy, χ is the GL-function mixing parameter, W_ν is the contribution to the Si 2s spectrum from the $SiN_\nu Si_{4-\nu}$ tetrahedra, $\nu = 0, 1, 2, 3, 4$, respectively. The W_ν values were selected from the best agreement between the experimental and calculated spectra. χ is 0.6 for irradiated Si_3N_4 and Si, and χ is 0.75 - for the initial Si_3N_4 sample. The deconvolution of the Si 2s spectrum of Si_3N_4 irradiated with B^+ ions showed that the main contribution to the Si 2s spectrum is made by the tetrahedra: $SiSi_4$, $SiSi_3N$ and SiN_4 (Fig. 2). The calculation indicates that the broadening of the Si 2s level upon irradiation with B^+ ions is associated with the formation of Si–Si bonds in Si_3N_4. If Si_3N_4 irradiated by B^+ ions with a higher fluence than further low-energy broadening of the Si2s spectrum can be expected.

The infrared transmission spectra of irradiated Si_3N_4 samples, before and after the annealing, are shown in Fig. 3. The transmission minimum of about 850 cm^{-1} for the initial Si_3N_4 sample indicated the Si–N bond. After the B^+ ion irradiation, the transmission minimum increased. The annealing is accompanied by the return of the spectra to the initial Si_3N_4 sample (Fig. 3).

The leakage current increases exponentially with the increase of electric field strength, both in the initial and in the irradiated samples. An increase in the irradiation fluence with B^+ ions is accompanied by an increase in the leakage current by two to three orders of magnitude. The annealing of nitride irradiated with B^+ ions leads to a decrease in the leakage current to a value corresponding to the leakage current of the initial unirradiated Si_3N_4 sample.

Fig. 4 is the dependence of current density on the electric field for silicon nitride irradiated with B^+ ions at different fluences.

An increase in temperature leads to an exponentially strong increase in the current density, both in the original samples and in the samples irradiated with B^+ ions (Fig. 5).

The experimental data on the current density dependence on the inverse temperature were simulated based on various charge transport models. The charge transport mechanism in a dielectric with traps is given by the expression [35]:

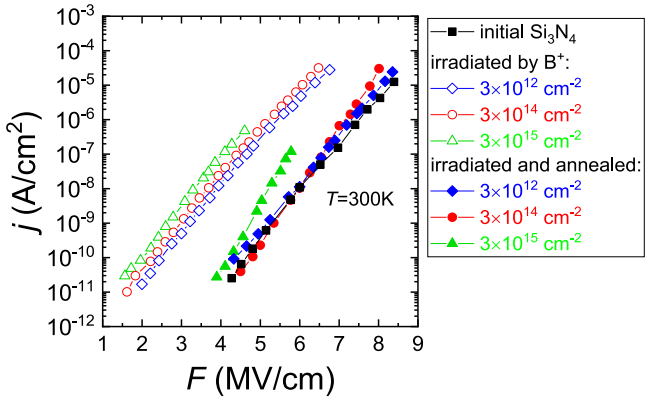

Fig. 4. Current density dependence on the electric field for Si_3N_4 irradiated with B^+ ions at different fluences. The ion energy of 100 keV with different fluences (3×10^{12} ion/cm^{-2}, 3×10^{14} ion/cm^{-2}, 3×10^{15} ion/cm^{-2}). The annealing of irradiated Si_3N_4 was carried out in a nitrogen atmosphere at 700 °C for 30 min.

$$j = \frac{e}{a^2}P = eN_t^{2/3}P. \quad (2)$$

Here, *j* – current density, *e* – electron charge, *a* – average distance between traps, $N_t = a^{-3}$ – trap concentration and *P* – trap ionization probability.

A one-dimensional monopolar model was used to describe the charge transport in Si_3N_4. The non-uniform electric field in Si_3N_4 was calculated using the Poisson equation. To model the leakage current in Si_3N_4, the following equations were solved numerically [36]:

$$\begin{cases} \dfrac{\partial n(x,t)}{\partial t} = \dfrac{1}{e}\dfrac{\partial j(x,t)}{\partial x} - \sigma\upsilon n(x,t)(N_t - n_t(x,t)) + n_t(x,t)P(x,t) \\ \dfrac{\partial n_t(x,t)}{\partial t} = \sigma\upsilon n(x,t)(N_t - n_t(x,t)) - n_t(x,t)P(x,t) \\ \dfrac{\partial F(x,t)}{\partial x} = -\dfrac{\partial^2 U(x,t)}{\partial x^2} = -e\dfrac{(n_t(x,t) + n(x,t))}{\varepsilon\varepsilon_0} \end{cases} \quad (3)$$

Here, *n(x,t)* and $n_t(x,t)$ are free and trapped electron concentrations, σ is the capture cross-section, ε is the low-frequency dielectric constant of Si_3N_4. *U(x,t)* and *F(x,t)* are the values of the local potential and electric field in Si_3N_4, respectively, υ is the charge drift velocity.

The boundary condition for the Poisson equation is the external voltage *U* value applied to the Al contact; for the equation describing the charge transport, the boundary condition was the injection current of electrons from the Si substrate, which was calculated based on the Fowler–Nordheim mechanism. The following parameter values were used for all models in the numerical simulation [36]: $\sigma = 5 \times 10^{-13}$ cm^2 and $\varepsilon = 7$, $\upsilon = 10^7$ cm/s.

The Frenkel model describes the Coulomb trap ionization in a strong electric field (Fig. 6). The trap ionization probability in Frenkel model is described by the expression [9,37]:

$$P_F = \nu \exp\left(-\frac{W - \left(\frac{e^3}{\pi\varepsilon_\infty\varepsilon_0}\right)^{1/2}\sqrt{F}}{kT} \right). \quad (4)$$

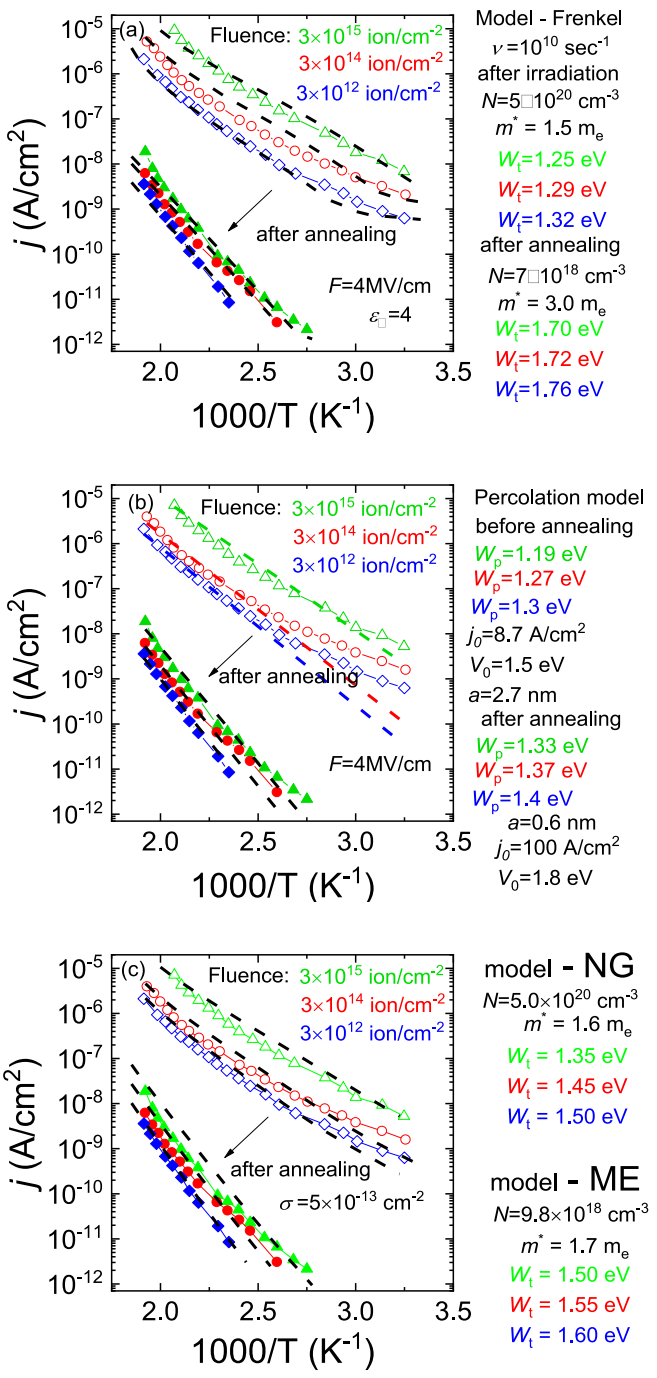

Fig. 5. Current density dependence of the inverse temperature for Si_3N_4 irradiated with B^+ ions and annealed-irradiated Si_3N_4 at an electric field strength of 4 MV/cm. Numerical dependences were calculated using (a) the Frenkel model with TAT, (b) Shklovskii-Efros percolation model, (c) the Makram-Ebeid and Lannoo model for annealed-irradiated Si_3N_4 and the Nasyrov-Gritsenko model of phonon-assisted tunneling between traps for Si_3N_4 irradiated with B^+ ions. The simulation parameters are shown in the figures.

Here, $\nu = W/h$ – attempt-to-escape factor, W – Coulomb trap ionization energy, h – Planck constant, $\varepsilon_\infty = n^2$ – high-frequency permittivity, n – refractive index, ε_0 – dielectric constant, F – electric field, k – Boltzmann constant and T – temperature.

For thermally assisted tunneling, the trap ionization probability has the form:

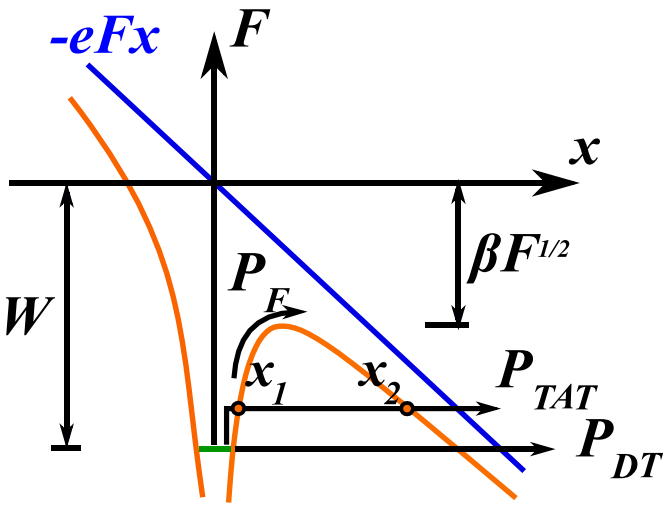

Fig. 6. Schematic representation of the Coulomb trap ionization in the Frenkel model taking into account thermally assisted tunneling (TAT).

$$P_{TAT} = \frac{\nu}{kT} \int_0^{W-\left(\frac{e^3}{\pi\varepsilon_\infty\varepsilon_o}\right)^{1/2}\sqrt{F}} \exp\left\{ -\frac{E}{kT} - \frac{2}{h}\int_{x_1}^{x_2} \sqrt{2m(eV(x)-E)}dx \right\} dE \quad (5)$$

$$V(x) = W - \frac{e}{4\pi\varepsilon_\infty\varepsilon_0 x} - Fx,$$

where ε – excited level energy, x_1, x_2 – classical turning points.

$$x_{1,2} = \frac{1}{2}\frac{W-E}{eF}\left(1 \mp \left(1 - \frac{eF}{\pi\varepsilon_\infty\varepsilon_0(W-E)^2}\right)^{1/2}\right) \quad (6)$$

P_{DT} is a direct tunneling trap ionization probability. In direct tunneling case, there is no temperature dependence. Therefore, the direct tunneling model is not applicable since, in the experimental data, the dependence on temperature does not disappear in the given temperature range (from 300K to 500K). A full trap ionization probability will be the sum of Frenkel trap ionization probability and a thermally assisted tunneling trap ionization probability ($P = P_F + P_{TAT}$).

The simulation of the current density dependence on the inverse temperature for Si_3N_4 irradiated with B^+ ions (Fig. 5 (a)) based on the Frenkel model yields the anomalously low attempt-to-escape factor value ($\nu = 10^{10}$ sec^{-1}). According to the Einstein equation $\nu = W/h$, the frequency factor value for the obtained trap energies is of the order of $\sim 10^{14}$ sec^{-1}, which is four orders of magnitude greater than the value obtained in the experiment. In addition, an anomalously large effective mass value for an electron was used in the calculations for the Frenkel effect with TAT. An anomalously large value of the effective mass of an electron was obtained in Ref. [36]. Thus, the Frenkel model does not describe the charge transport mechanism in B^+-ion irradiated nitride before and after annealing.

The charge transport in an irradiated semiconductor can be described by the percolation theory. The charge transport in a non-periodic fluctuating potential is described by the Shklovskii-Efros percolation model [38,39]. This model assumes that excited electrons with an energy exceeding the percolation energy move around a random potential (Fig. 7). The Shklovskii-Efros percolation model of large-scale potential fluctuations in a heavily doped compensated semiconductor is illustrated in Fig. 7(a). According to this model, the semiconductor bandgap is constant, and potential fluctuations are caused by a nonuniform spatial distribution of charged (ionized) donors and acceptors. The formation of electron-hole pairs is accompanied by their

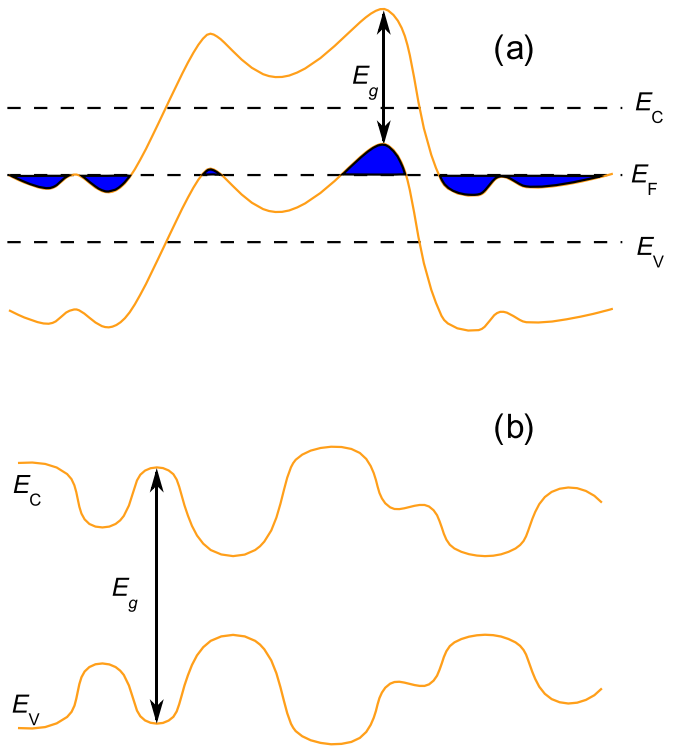

Fig. 7. (a) Model of large-scale potential fluctuations. (b) Model of large-scale band gap fluctuations.

spatial separation, which does not promote the recombination of electrons and holes. In Fig. 7(b) is a model of large-scale potential fluctuations, caused by variations in the local chemical composition, illustrated by a one-dimensional diagram.

The current density in the percolation model is given by the expression [38,39]:

$$j = j_0 \exp\left(-\frac{W_p - \left(CeFa_pV_0^{\gamma}\right)^{\frac{1}{1+\gamma}}}{kT}\right), \tag{7}$$

Here, j_0 is the pre-exponential factor, W_p is the percolation energy, $C \approx 0.25$ is a numerical constant, e is the electron charge, F is the electric field, a_p is the spatial scale of fluctuations, V_0 is the amplitude of energy fluctuations and γ is the critical index equal to 0.9.

The Shklovskii-Efros percolation model considers only thermal excitations in a large-scale potential. This model does not take into account the tunneling possibility. The classical criterion for the percolation model applicability is the absence of tunneling effect. In our case, the absence of the tunneling effect is indicated by the strong current density dependence on temperature.

For the Shklovskii-Efros model after the irradiation and a subsequent annealing of Si_3N_4, the spatial fluctuation scale value estimated from Fig. 5(b) for different irradiation fluences was 0.6 nm. Since the tunneling probability at such a spatial scale is high, the criterion for the classical applicability of this model is not satisfied for annealed-irradiated Si_3N_4. The spatial fluctuation scale value for irradiated Si_3N_4 for all three fluences is 2.7 nm. With this spatial scale value, the tunneling probability is small and the model can be applied.

The Shklovskii-Efros model describes the current density dependences on the inverse temperature for the radiation fluence of 3×10^{15} ion/cm^{-2} from 500 K to 340 K. For the radiation fluence of 3×10^{15} ion/cm^{-2} from 340 K to 300 K, the experimental and theoretical curves diverge. The percolation theory predicts a fixed activation energy, while, in the experiment, a deviation of the experiment from a linear dependence in the $lg\ j$-$1000/T$ coordinates is observed. For irradiation fluences 3×10^{12} ion/cm^{-2} and 3×10^{14} ion/cm^{-2}, the theoretical curves, according to the Shklovskii-Efros model, describe well the temperature range from 500K to 400K and completely diverge from the experimental curves at temperatures below 400 K. Therefore, the Shklovskii-Efros percolation model only partially describes the experimental data on the current density from the inverse temperature in irradiated Si_3N_4. The Shklovskii-Efros percolation model does not describe the charge transport in irradiated and annealed Si_3N_4.

The Makram-Ebeid and Lannoo model of multiphonon isolated trap ionization describes the charge transport of an isolated neutral trap [12]. In Fig. 8(a) is the configuration diagram of the trap in the ground (black curve) and excited (red curve) states. The potential black curve corresponds to the case when an electron is captured in the trap, and the red curve – to the case of an empty trap. Here, W_{opt} is the optical ionization energy of a trap and W_t is the thermal ionization energy. As can be seen in Fig. 8(a), two trap ionization ways are possible. In the first case, the transition from the ground state to the excited state is carried out due to the vertical transition (W_{opt}). In the second case, the excitation occurs via an indirect transition (W_t). As a rule, an isolated trap ionization occurs due to the phonon absorption.

In the multiphonon trap ionization, an electron tunnels into the conduction band. The free electron moves in the electric field direction until it is captured by the next trap. During the trap ionization, the electron movement in the conduction band proceeds until it is captured by another trap and continues until the electron reaches the opposite contact (Fig. 8 (b)) [12]. This mechanism is typical of the case of a low trap concentration (Nt $< 10^{19}$ cm^{-3}).

In the Macram-Ebeid and Lannoo model of multiphonon isolated trap ionization, the ionization probability has the form [12]:

$$P = \sum \exp\left(\frac{nW_{ph}}{2kT} - \frac{W_{opt} - W_t}{W_{ph}} \coth\frac{W_{ph}}{2kT}\right) I_n\left(\frac{W_{opt} - W_t}{W_{ph}\sinh\left(W_{ph}/2kT\right)}\right) P_i, \tag{8}$$

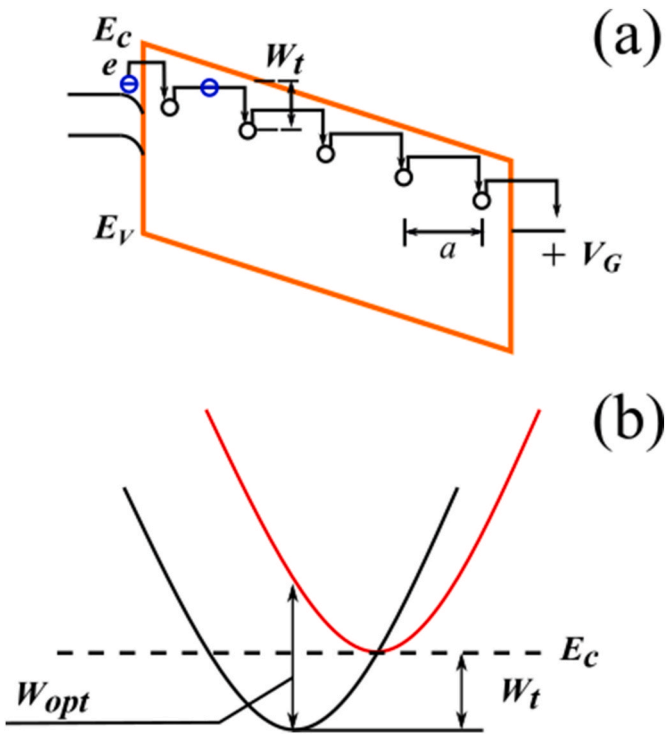

Fig. 8. (a) Schematic representation of multiphonon neutral isolated trap ionization according to the Makram-Ebeid and Lannoo model. (b) Configuration diagram of the trap in the Makram-Ebeid and Lannoo model.

$$P_i = \frac{eF}{2\sqrt{2m^*(W_t + nW_{ph})}} \exp\left(-\frac{4}{3}\frac{\sqrt{2m^*}}{\hbar eF}(W_t + nW_{ph})^{3/2} \right). \quad (9)$$

Here, W_t – thermal trap ionization energy, W_{opt} – optical trap ionization energy W_{ph} – phonon energy, I_n – modified Bessel function, P_i – tunneling probability through a triangular barrier and ħ – reduced Planck constant.

The Makram-Ebeid and Lannoo model does not describe the charge transport in Si_3N_4 irradiated with B^+ ions due to the anomalously high effective mass value ($m^* = 6.5\ m_e$) obtained from the calculations. The Makram-Ebeid and Lannoo model satisfactorily describes the charge transport in Si_3N_4 after irradiation and the subsequent annealing. The simulation results of the current density dependence on the inverse temperature using the Makram-Ebeid and Lannoo model for Si_3N_4 after irradiation and the subsequent annealing are shown in Fig. 5 (c). The trap concentration in Si_3N_4 after irradiation and the subsequent annealing obtained from the simulation is 9.8×10^{18} cm^{-3}. The simulated parameters for the annealed-irradiated Si_3N_4 sample are comparable with the simulated parameters for pyrolytic Si_3N_4 [40].

In the high trap concentration case, $N_t > 10^{19}$ cm^{-3}, the distance between the traps becomes small, and it becomes advantageous for an electron after the ionization from a trap to tunnel to a neighboring trap without entering the conduction band (Fig. 9(a)). In this case, the electron is ionized due to the absorption of a large number of phonons from the ground state of the "filled" trap ($U_b(Q)$) to its excited state ($U_f(Q)$), then tunnels to the excited state of the neighboring "empty" trap, after which the relaxation to the ground state of this trap occurs (Fig. 9(b)). The charge transport at a high trap concentration is described in the Nasyrov-Gritsenko model of phonon-assisted tunneling between neighboring traps [14]. The trap ionization probability in this model is determined by the expression [14]:

$$P = \int \frac{\hbar|E|}{m^* a^2 kTQ_0} \exp\left\{ -\left(\frac{(Q-Q_0)^2 + (Q - eFa/Q_0)^2}{2kT} - \frac{4\sqrt{2m^*}}{3\hbar eF}\left[(-E)^{3/2} - (-E - eFa)^{3/2}\right] \right) \right\} dQ, \quad (10)$$

where $E = -Q_0(Q - Q_0) - W_{opt}$, $Q_0 = \sqrt{2(W_{opt} - W_t)}$, Q is the oscillator coordinate

If the localization length of a trapped electron is comparable with the separation between traps and the conditions $kT \ll W_t$ and $eFa \ll W_t$ are met, then expression 10 can be rewritten in the analytical form [14]:

$$P = \frac{2\sqrt{\pi}\hbar W_t}{m^* a^2 \sqrt{2kT(W_{opt} - W_t)}} \exp\left(-\frac{W_{opt} - W_t}{kT} \right) \exp\left(-\frac{2a\sqrt{2m^* W_t}}{\hbar} \right) \sinh\left(\frac{eFa}{2kT} \right) \quad (11)$$

The irradiation of Si_3N_4 leads to an increase in the leakage current, which indicates an increase in the trap concentration; this conclusion is confirmed by the numerical simulation (Fig. 5(c)). The trap concentration, according to the simulation result of Nasyrov-Gritsenko model, is 5.0×10^{20} cm^{-3}. Depending on the B^+ ion irradiation fluence, the differences in leakage currents are explained by the ionization energy change from 1.5 eV at a fluence of 3×10^{12} ion/cm^{-2} to 1.35 eV at a fluence of 3×10^{15} ion/cm^{-2}. The Nasyrov-Gritsenko model does not describe the charge transport mechanism of Si_3N_4 after the annealing of irradiated samples since a quantitative agreement between the experimental data and the theoretical model data was reached at a trap concentration not characteristic for the initial Si_3N_4 sample ($N_t = 2.4 \times 10^{20}$ cm^{-3}) [42]. The Nasyrov-Gritsenko model describes the charge transport mechanism in Si_3N_4 irradiated with B^+ ions with reasonable parameters of trap concentration and trap ionization energies.

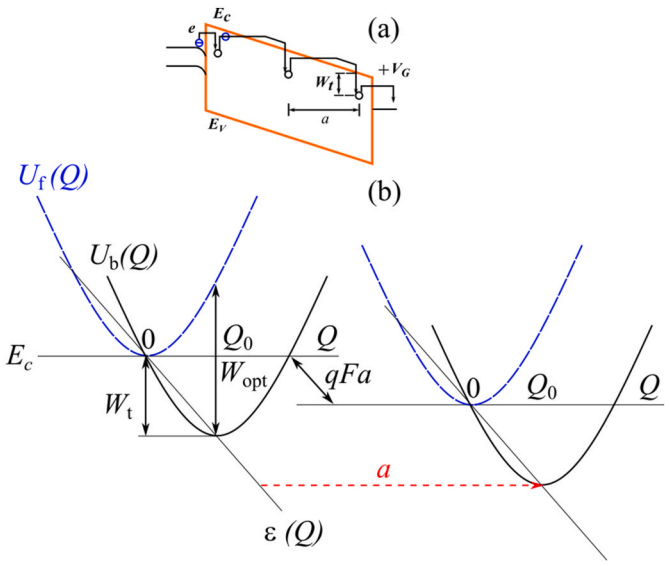

Fig. 9. (a) Schematic representation of multiphonon trap ionization according to the Nasyrov-Gritsenko model of phonon-assisted tunneling between neighboring traps. (b) Configuration diagram of the Nasyrov-Gritsenko model.

4. Conclusion

The effect of B^+ ion irradiation on the charge transport in amorphous Si_3N_4 was studied. The B^+ ion irradiation increased leakage currents by two to three orders of magnitude. The annealing in a nitrogen atmosphere at 700 °C decreased leakage currents to their initial values. It can be assumed that the increase in leakage currents during irradiation is due to radiation defects. These defects are annealed. The charge transport mechanism is described within the multiphonon models. The Nasyrov-Gritsenko model of phonon-assisted tunneling between neighboring traps describes the charge transport mechanism in B^+-irradiated Si_3N_4 at a high trap concentration. The Makram-Ebeid and Lannoo model of multiphonon isolated trap ionization describes the charge transport in B^+-irradiated Si_3N_4 after annealing. The ionization trap energy in the initial Si_3N_4 sample and annealed-irradiated Si_3N_4 sample lies in the range from 1.5 eV to 1.6 eV.

CRediT authorship contribution statement

V.A. Gritsenko: Writing – review & editing, Writing – original draft, Validation, Supervision, Resources, Project administration, Investigation, Funding acquisition, Conceptualization. **Yu N. Novikov:** Writing – review & editing, Writing – original draft, Visualization, Validation, Methodology, Formal analysis. **A.A. Gismatulin:** Writing – review & editing, Writing – original draft, Visualization, Validation, Methodology, Formal analysis.

Declaration of competing interest

The authors declare that they have no known competing financial interests or personal relationships that could have appeared to influence the work reported in this paper.

Acknowledgment

The work was supported by the Russian Science Foundation, grant №25-12-00022.

Data availability

Data will be made available on request.

References

[1] K.J. Rietwyk, Y. Smets, M. Bashouti, S.H. Christiansen, A. Schenk, A. Tadich, M. T. Edmonds, J. Ristein, L. Ley, C.I. Pakes, Charge transfer doping of silicon, Phys. Rev. Lett. 112 (2014) 155502.

[2] M. Wang, A. Debernardi, Y. Berencén, R. Heller, C. Xu, Y. Yuan, Y. Xie, R. Böttger, L. Rebohle, W. Skorupa, M. Helm, S. Prucnal, S. Zhou, Breaking the doping limit in silicon by deep impurities, Phys. Rev. Appl. 11 (2019) 054039.

[3] S.M. Sze, Physics of Semiconductor Devices, John Wiley & Sons, Taiwan, 1981.

[4] C.-H. An, M.S. Lee, J.-Y. Choi, H. Kim, Change of the trap energy levels of the atomic layer deposited HfLaOx films with different La concentration, Appl. Phys. Lett. 94 (2009) 262901.

[5] D.S. Jeong, C.S. Hwang, Tunneling current from a metal electrode to many traps in an insulator, Phys. Rev. B 71 (2005) 165327.

[6] A.S. Foster, L. Gejo, A.L. Shluger, R.M. Nieminen, Vacancy and interstitial defects in hafnia, Phys. Rev. B 65 (2002) 174117.

[7] V.A. Gritsenko, E.E. Meerson, Yu N. Morokov, Thermally assisted hole tunneling at the Au-Si3N4 interface and the energy-band diagram of metal-nitride-oxide-semiconductor structures, Phys. Rev. B 57 (1998) R2081–R2083.

[8] G. Jegert, A. Kersch, W. Weinreich, U. Schröder, P. Lugli, Modeling of leakage currents in high-dielectrics: three-dimensional approach via kinetic Monte Carlo, Appl. Phys. Lett. 96 (2010) 062113.

[9] J. Frenkel, On pre-breakdown phenomena in insulators and electronic Semi-conductors, Phys. Rev. B 54 (1938) 647–648, https://doi.org/10.1103/PhysRev.54.647.

[10] K.A. Nasyrov, V.A. Gritsenko, Transport mechanisms of electrons and holes in dielectric films, Phys. Usp. 56 (2013) 999–1012, https://doi.org/10.3367/UFNe.0183.201310h.1099.

[11] A.A. Gismatulin, YuN. Novikov, N.V. Andreeva, D.S. Mazing, V.A. Gritsenko, Origin of exponentially large increase in the leakage current in alumina films depending on the ALD synthesis temperature, Appl. Phys. Lett. 125 (2024) 062901, https://doi.org/10.1063/5.0217150.

[12] S.S. Makram-Ebeid, M. Lannoo, Quantum model for phonon-assisted tunnel ionization of deep levels in a semiconductor, Phys. Rev. B 25 (1982) 6406, https://doi.org/10.1103/PhysRevB.25.6406.

[13] YuN. Novikova, V.A. Gritsenko, Multiphonon trap ionization mechanism in amorphous SiNx, J. Non-Cryst. Solids 582 (2022) 121442.

[14] K.A. Nasyrov, V.A. Gritsenko, Charge transport in dielectrics via tunneling between traps, J. Appl. Phys. 109 (2011) 093705.

[15] William L. Warren, P.M. Lenahan, Sean E. Curry, First observation of paramagnetic nitrogen dangling-bond centers in silicon nitride, Phys. Rev. Lett. 65 (1990) 207–210.

[16] D.T. Krick, P.M. Lenahan, Nature of the dominant deep traps in amorphous silicon nitride? Phys. Rev. B 38 (1988) 8226.

[17] W.L. Warren, P.M. Lenahan, Electron-nuclear double-resonance and electron-spin-resonance study of silicon dangling-bond center in silicon nitride, Phys. Rev. B 42 (1990) 1773–1780.

[18] W.L. Warren, J. Kanicki, J. Robertson, E.H. Poindexter, P.J. McWhorter, Electron paramagnetic resonance investigation of charge trapping centers in amorphous silicon nitride films, J. Appl. Phys. 74 (1993) 4034–4046.

[19] V.A. Gritsenko, J.B. Xu, I.H. Wilson, R.M. Kwok, Y.H. Ng, Short range order and nature of defects and traps in amorphous silicon oxynitride, Phys. Rev. Lett. 81 (1998) 1054–1057.

[20] L. Hückmann, J. Cottom, J. Meyer, Intrinsic charge trapping and reversible charge induced structural modifications in a-Si3N4, Adv. Physics Res. 3 (2024) 2300109.

[21] V.A. Gritsenko, N.V. Perevalov, O.M. Orlov, G. Ya Krasnikov, Nature of traps responsible for the memory effect in silicon nitride, Appl. Phys. Lett. 109 (2016) 06294, https://doi.org/10.1063/1.4959830.

[22] Yu N. Novikov, V.A. Gritsenko, Charge transport mechanism and amphoteric nature of traps in amorphous silicon nitride, J. Non-Cryst. Solids 544 (2020) 120186.

[23] C. Wilhelmer, D. Waldhör, L. Cvitkovich, D. Milardovich, M. Waltl, T. Grasse, Polaron formation in the hydrogenated amorphous silicon nitride Si3N4:H, Phys. Rev. B 110 (2024) 045201.

[24] V.A. Gritsenko, Silicon nitride on si: electronic structure for flash memory devices, in: V. Narayanan, M. Frank, A. Demkov (Eds.), Thin Films on Silicon: Electronic and Photonic Applications, World Scientific Press, 2016, pp. 273–322.

[25] A. Goda, Recent progress on 3D NAND flash technologies, Electronics 10 (2021) 3156.

[26] G. Li, H. San, Xu-yuan Chen, Charging and discharging in ion implanted dielectric films used for capacitive radio frequency microelectromechanical systems switch, J. Appl. Phys. 105 (2009) 124503.

[27] Y. Yu, W. Li, P. Wu, C. Jiang, X. Xiao, Gate dielectric ion implantation to modulate the threshold voltage of In2O3 nanowire field effect transistors, Appl. Phys. Lett. 109 (2016) 193505.

[28] D. Rao, O. Chowdhury, A.I.K. Pillai, G.K. Pradhan, S. Sahoo, J.P. Feser, M. Garbrecht, B. Saha, Multifunctional irradiation-induced defects for enhancing thermoelectric properties of scandium nitride thin films, ACS Appl. Energy Mater. 5 (2022) 6847–6854.

[29] R. Burcea, H. Bouteiller, S. Hurand, P. Eklund, J.-F. Barbot, A. le Febvrier, Effect of induced defects on conduction mechanisms of noble-gas-implanted ScN thin films, J. Appl. Phys. 134 (2023) 055107.

[30] Z. Zhao, L. Yang, Y. Feng, D. Min, P. Zhai, J. Liu, S. Li, Monoclinic-to-tetragonal transition in HfO2 induced by swift heavy ions: effects of thermal spike and oxygen defects, Acta Mater. 254 (2023) 118992.

[31] A.A. Gismatulin, V.A. Gritsenko, Exponentially strong leakage current increase in the proton-irradiated silicon nitride, Scr. Mater. 270 (2026) 116968.

[32] http://xpsdatabased/silicon-si-z14.

[33] I. Hoflijk, A. Vanleenhove, I. Vaesen, C. Zborowski, K. Artyushkova, T. Conard, HAXPES spectra of Si_3N_4 measured by Cr Kα, Surf. Sci. Spectra 29 (2022) 014013 https://doi.org/10.1116/6.0001524.

[34] V. Jaina, M.C. Biesingerb, M.R. Linford, The Gaussian-Lorentzian Sum, product, and convolution (Voigt) functions in the context of peak fitting X-ray photoelectron spectroscopy (XPS) narrow scans, Appl. Surf. Sci. 447 (2018) 548–553, https://doi.org/10.1016/j.apsusc.2018.03.190.

[35] V.A. Gritsenko, T.V. Perevalov, V.A. Voronkovskii, A.A. Gismatulin, V. N. Kruchinin, V. Sh Aliev, V.A. Pustovarov, I.P. Prosvirin, Y. Roizin, Charge transport and the nature of traps in oxygen deficient tantalum oxide, ACS Appl. Mater. Interfaces 10 (2018) 3769–3775, https://doi.org/10.1021/acsami.7b16753.

[36] K.A. Nasyrov, V.A. Gritsenko, M.K. Kim, H.S. Chae, S.D. Chae, W.I. Ryu, J.H. Sok, J.-W. Lee, B.M. Kim, Charge transport mechanism in metal–nitride–oxide–silicon structures, IEEE Electron Device Lett. 23 (2002).

[37] J. Frenkel, On the theory of electric breakdown of dielectrics and electronic semiconductors, Technical Physics of the USSR 5 (1938) 685–695.

[38] B.I. Shklovskii, Percolation electrical conductivity in strong electric field, Sov. Phys. Semiconduct. 13 (1979) 53–56.

[39] B.I. Shklovskii, A.L. Efros, Percolation theory and conductivity of strongly inhomogeneous media, Usp. Fiz. Nauk 117 (1975) 401–435.

[40] Yu N. Novikov, V.A. Gritsenko, Multiphonon trap ionization mechanism in amorphous SiNx, J. Non-Cryst. Solids 582 (2022) 121442, https://doi.org/10.1016/j.jnoncrysol.2022.121442.